Inorg. Chem. **2005**, *44*, 3233–3240

Structural Variability and Dynamics in Carboxylato- and Carbamatomagnesium Bromides. Relationship to the Carboxylate Shift

M. Tyler Caudle,*,† William W. Brennessel,‡ and Victor G. Young, Jr.‡

Department of Chemistry and Biochemistry, Arizona State University, Tempe, Arizona 85287-1604, and Department of Chemistry, University of Minnesota, Minneapolis, Minnesota 55455

Received November 5, 2004

Two new carbamatomagnesium bromide complexes **1** (=$[Mg(O_2CN(Me)Ph)(THF)_2Br]_2$) and **2** (=$[Mg_3(O_2CNPh_2)_4(THF)_5Br][(THF)MgBr_3]$) were prepared and crystallographically characterized. Complex **1** consists of a dinuclear core with two syn-syn-$\mu_{1,3}$ bridging carbamato ligands. In solution, the ^1H and ^{13}C NMR spectra revealed a two-site fluxional behavior for the carbamato ligands between 0 °C and 25 °C that is consistent with a bridge-mode isomerization relating the syn-syn-$\mu_{1,3}$ form and an alternative syn-anti-$\mu_{1,1}$ form. At temperatures below 0 °C, a more complex NMR signal is observed that is ascribed to further resolution of C–N rotational isomers, which has the effect of increasing the number of molecular isomers that can be resolved on the NMR time scale. New temperature-dependent NMR spectra of the previously known diethylcarbamato- and benzoato-bridged complexes $[Mg(O_2CNEt_2)(THF)_2Br]_2$, **3**, and $[Mg(O_2CPh)(THF)_2Br]_2$, **5**, revealed fluxional behavior that was also interpreted in terms of bridge-mode isomerization. Kinetic activation parameters for **1**, **3**, and **5** are consistent with an intramolecular motion relating the syn-syn-$\mu_{1,3}$ and syn-anti-$\mu_{1,1}$ isomers. These results provide new insight into bridge-mode isomerism that is closely related to the carboxylate shift concept. Complex **2** is compositionally related to **1** but exists as a salt consisting of a trinuclear cationic unit $[Mg_3(O_2CNPh_2)_4(THF)_5Br]^+$ and a solvated tribromomagnesiate anion $[(THF)MgBr_3]^-$. This shows that changing the hydrocarbon substitutents on the carbamato ligand changes the structure and dynamics of multinuclear carbamatomagnesium complexes in ways that limit our ability to predict structural topologies in this system.

Introduction

Reactions that involve addition of carbon dioxide to metal−nitrogen bonds are of interest for their potential in generating new chelating functional groups for metal ions.[1] Recent work has demonstrated the utility of formal CO_2 insertion into Mg−N bonds to generate carbamatomagnesium complexes of considerable structural and topological variety.[2−5] Addition of CO_2 to amidomagnesium bromides or alkylmagnesium bromides gives carbamato- or carboxylatomagnesium bromides of the empirical formula $[Mg(O_2CR)(L)_2Br]_n$. Known compounds of this type have a solvated dinuclear structure in which two magnesium ions are bridged by two carbamato or carboxylato ligands and are solvated by four solvent molecules L, Scheme 1 (R = **3**, $-NEt_2$; **4**, $-N^iPr_2$; **5**, $-C_6H_5$).[3−5] These compounds exist as one of two bridge-mode isomers. A syn-syn-$\mu_{1,3}$ bridging mode is correlated with a long Mg−Mg distance of greater than 3.7 Å and an Mg−O distance *B* greater than 3.0 Å, Scheme 2. An alternative syn-anti-$\mu_{1,1}$ bridging mode results in a shortened Mg−Mg distance of less than 3.4 Å and Mg−O distance *B* smaller than 2.5 Å. We previously reported that compound **3** exhibited both coordination modes in the solid state, and in solution the two isomers were shown to be related by a dynamic process that could be resolved at low temperature.[5] However, no kinetic parameters were reported

* To whom correspondence should be addressed.
† Arizona State University.
‡ University of Minnesota.

(1) Walther, D.; Ruben, M.; Rau, S. *Coord. Chem. Rev.* **1999**, *182*, 67−100. Belli Dell'Amico, D.; Calderazzo, F.; Labella, L.; Marchetti, F.; Pampaloni, G. *Chem. Rev.* **2003**, *103*, 3857−3897.
(2) Caudle, M. T.; Nieman, R. A.; Young, V. G., Jr. *Inorg. Chem.* **2001**, *40*, 1571−1575. Tang, Y.; Zakharov, L. N.; Rheingold, A. L.; Kemp, R. A. *Organometallics* **2004**, *23*, 4788−4791.
(3) Yang, K.-C.; Chang, C.-C.; Yeh, C.-S.; Lee, G.-H.; Peng, S.-M. *Organometallics* **2001**, *20*, 126−137.
(4) Ruben, M.; Walther, D.; Knake, R.; Gorls, H.; Beckert, R. *Eur. J. Inorg. Chem.* **2000**, 1055−1060.
(5) Caudle, M. T.; Kampf, J. W. *Inorg. Chem.* **1999**, *38*, 5474−5475.

10.1021/ic048442p CCC: $30.25
Published on Web 03/30/2005

Scheme 1

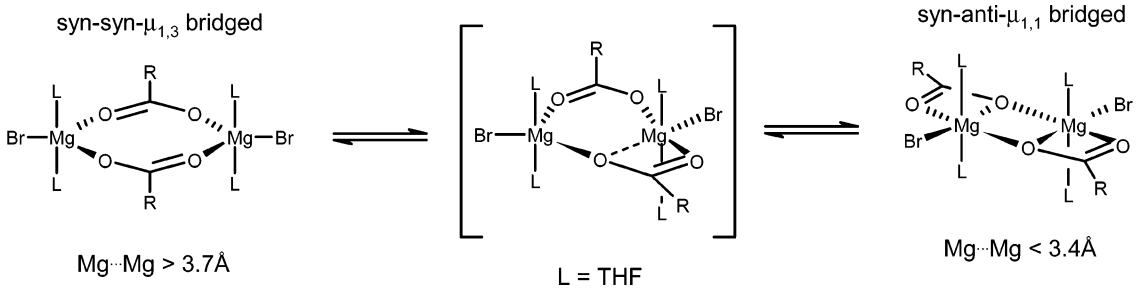

Scheme 2

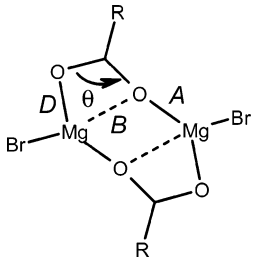

in this preliminary communication, and so no inference concerning the mechanism for bridge mode isomerization could be made.

The bridge-mode isomerism exhibited by this class of compounds is closely related to the carboxylate shift concept, as delineated by Rardin et al.[6] This concept correlates the structural parameters in Scheme 2 for a broad group of carboxylato-bridged compounds. The concept is applied in understanding static crystal structures of dinuclear enzyme active sites, and dynamic shifts between carboxylate-shift bridge-mode isomers are commonly invoked as a means by which coordination sites may be opened in the mechanism for these enzymes.[7−10] However, there is only one prior paper reporting kinetic and activation parameters for this type of bridge-mode isomerization,[11] and no such prior reports on dinuclear systems. This is an important issue since X-ray structures of dinuclear carboxylato-bridged complexes and proteins present a static representation of the structure in the solid state that may incompletely represent the full range of structural minima in solution. The dinuclear biological systems of interest involve paramagnetic iron or manganese centers that complicate analysis of structural dynamics by NMR spectroscopy. Diamagnetic magnesium complexes of the type illustrated in Scheme 1 offer the unique opportunity to measure such dynamics in a simple dinuclear system using nuclear magnetic resonance in order to assess the fundamental importance of bridge-mode isomerization in solution.

For carbamato-bridged magnesium complexes, prior work shows that the nature of the groups on nitrogen can have a considerable impact on the structure and topology of carbamatomagnesium complexes. The hexanuclear compound $Mg_6(O_2CNEt_2)_{12}$ exists as a helical D_2 symmetric cluster, but substitution of phenyl groups for ethyl gives a compositionally related cluster $Mg_6(O_2CNPh_2)_{12}$ that exists as a D_3 symmetric ring.[3] This flexibility arises due to the lack of any crystal field preferences for the Mg^{2+} ion. As a result, the structural chemistry of magnesium carbamato complexes is rich and can be affected by subtle changes in the carbamato ligand. This is especially true when secondary coordinating anions such as halides are present. In this paper we report on the synthesis and structural characterization of two new carbamatomagnesium bromides derived from aromatic amines. The first new compound $[Mg(O_2CN(CH_3)Ph)Br][THF]_2$, **1**, exists as a solvated dimer that clearly belongs to the class of dinuclear carbamatomagnesium bromides shown in Scheme 1. We measured bridge-mode dynamics for this compound along with dynamics for two related dinuclear complexes whose structures were previously reported in the literature.[3,5] These three compounds now constitute the only examples of dinuclear compounds where activation parameters have been reported for a carboxylate-shift-like bridge-mode isomerization reaction. The diphenyl derivative $[Mg(O_2CNPh_2)Br][THF]_{1.5}$, **2**, adopts an entirely different and heretofore unprecedented ate-type structure consisting of discrete solvated $[Mg_3(O_2CNPh_2)_4Br]^+$ cations and solvated $[MgBr_3]^-$ anions, which illustrates the importance of the amino group in dictating the overall complex topology in the solid state and in solution. Despite their differences, compounds **1** and **2** have identical metal/ligand compositions, highlighting the difficulty in obtaining predictable topologies in the carbamatomagnesium systems generated by addition of CO_2 to Mg−N bonds.

Experimental Section

Materials and Methods. *N*-Methylaniline, diphenylamine, methylmagnesium bromide, and phenylmagnesium bromide were obtained from Aldrich and used as received. $^{13}CO_2$ was obtained from Cambridge Isotope laboratories. Compounds **3**−**5** were prepared and characterized as described in prior literature.[3−5] All preparations and manipulations were carried out under a nitrogen atmosphere in a glovebox or using standard Schlenk techniques. Room-temperature NMR spectra were measured on a Gemini 300 MHz

(6) Rardin, L.; Tolman, W. B.; Lippard, S. J. *New. J. Chem.* **1991**, *15*, 417−430.
(7) Andersson, M. E.; Högbom, M.; Rinaldo-Matthis, A.; Andersson, K. K.; Sjöberg, B.; Nordlund, P. *J. Am. Chem. Soc.* **1999**, *121*, 2346−2352.
(8) Nordlund, P.; Eklund, H. *J. Mol. Biol.* **1993**, *232*, 123−164.
(9) Högbom, M.; Andersson, M. E.; Nordlund, P. *J. Biol. Inorg. Chem.* **2001**, *6*, 315−323.
(10) Rosenzweig, A. C.; Nordlund, P.; Takahara, P. M.; Frederick, C. A.; Lippard, S. J. *Chem. Biol.* **1995**, *2*, 409−418. Gherman, B. F.; Baik, M.-H.; Lippard, S. J.; Friesner, R. A. *J. Am. Chem. Soc.* **2004**, *126*, 2978−2990. Guallar, V.; Gherman, B. F.; Lippard, S. J.; Friesner, R. A. *Curr. Opin. Chem. Biol.* **2002**, *6*, 236−242; Whittington, D. A.; Lippard, S. J. *J. Am. Chem. Soc.* **2001**, *123*, 827−838.
(11) Demšar, A.; Košmrlj, J.; Petricek, S. *J. Am. Chem. Soc.* **2002**, *124*, 3951−3958.

instrument. Temperature-dependent NMR spectra were measured on a Varian Inova 400 MHz instrument or a Varian Inova 500 MHz instrument.

$[Mg(O_2CN(Me)Ph)(THF)_2Br]_2$ (1). *N*-methylaniline (1.6 mL, 15 mmol) was dissolved in 75 mL of anhydrous THF and reacted with 5.0 mL (15 mmol) of methylmagnesium bromide (3.0 M solution in diethyl ether). After 30 min, the solution was sparged with dry carbon dioxide gas for 10 min at 1 atm and allowed to stand overnight under 1 atm CO_2. The resulting white powder was collected by filtration and washed with clean THF. The complex was dissolved in methylene chloride and an excess of THF was added. After standing overnight, the resulting white powder was collected. This gave a purified yield of 4.17 g (87%) of **1** as a white microcrystalline powder. X-ray quality crystals were prepared by slow evaporation of a solution of **1** in CH_2Cl_2/THF. Anal. Found-(calcd)%: C, 46.3(46.4); H, 6.0(5.5); N, 3.9(3.9). ^{1}H NMR ppm (H): 7.25 (broad, 4H), 7.12 (broad, 1H), 3.73 (broad, 8H), 3.30 (broad, 3H), 1.78 (broad, 8H). ^{13}C NMR ppm: 161.5 (broad, $-CO_2$), 128.5 (phenyl), 125.7 (phenyl), 68.8 (THF), 25.4 (THF). A ^{13}C enriched complex was prepared by substituting $^{13}CO_2$ for CO_2 and decreasing the scale of the reaction by a factor of 10.

$[Mg_3(O_2CNPh_2)_4(THF)_5Br][(THF)Mg(Br)_3]\cdot THF$ (2). Diphenylamine (2.54 g, 15 mmol) was dissolved in 75 mL of anhydrous THF and deaerated with a stream of N_2. Then 5.0 mL (15 mmol) of methylmagnesium bromide (3.0 M solution in diethyl ether) was added under N_2 to give a pale brown solution. After 30 min the solution was sparged with dry carbon dioxide gas at 1 atm. The solution almost immediately became pale yellow. After 30 min, the solvent was removed by evacuation to give a light yellow powder. Recrystallization from toluene gave a purified yield of 2.96 g (44.6%) of **2** as a white powder. ^{1}H NMR ppm (H): 7.28 (broad, 10 H) 3.62 (broad, 4H), 1.78 (broad, 4H). ^{13}C NMR ppm: 159.8 ($-CO_2$), 159.3 ($-CO_2$), 128.5 (phenyl), 127.3 (phenyl), 125.7 (phenyl), 68.3 (THF), 25.1 (THF). Anal. Found(calcd)%: C, 54.1-(54.3); H, 6.1(5.4); N, 3.2(3.8). Crystals for X-ray diffraction were grown from the filtrate used for recrystallization.

Crystallography. Suitable crystals of **1** and **2** were mounted on glass fibers for data collection at 173 K on a Siemens SMART Platform CCD diffractometer using Mo Kα radiation. The specimen used to determine the crystal structure of **1** was a nonmerohedral twin. The twin operation was determined to be a 180° rotation about [001] in reciprocal space to yield the twin law (by rows) [−1 0 0/0 −1 0/0.303 −0.848 1].[12] The raw data were integrated with SAINT V6.45.[13] An absorption and scaling correction was applied with TWINABS V1.02.[14] For **2**, a single crystal was measured in the normal way having the data integrated with SAINT V6.01[13] and an absorption and scaling correction applied with SADABS V1.0.[14] 499 redundant reflections were removed, leaving 5541 unique reflections with STRIP REDUNDANT V1.3.[15] Both structures were solved and refined using SHELXTL V6.12.[16] Solution of **1** was straightforward. A direct-methods solution provided most non-hydrogen atoms, and the full-matrix least-squares/difference Fourier cycling located the remaining non-hydrogen atoms. Non-hydrogen atoms were refined with anisotropic displacement parameters and hydrogen atoms placed in ideal positions as riding atoms and refined with isotropic displacement parameters. This structure refined to R1 = 0.0439 and wR2 = 0.0759 (F^2, all data). In **2**, the coordinated THF solvent molecules and the uncoordinated THF solvent molecule were highly disordered. They were modeled as disordered over two positions each with many geometrical and thermal restraints and constraints. The $[(THF)MgBr_3]^-$ anion was also disordered and modeled over two positions. Two residual peaks of electron density (approximately one electron per Å^3 each) were located near a Br atom and near the uncoordinated THF solvent molecule; the former is likely due to Fourier truncation, and the latter was likely due to additional disorder of the THF solvent molecule that could not be modeled. Thus, this structure was refined to R1 = 0.0767 and wR2 = 0.1520 (F^2, all data). Refer to Table 1 for details of the crystal data and refinement for both compounds.

Table 1. Crystallographic Data for **1** and **2**

	1	**2**
formula	$C_{16}H_{24}BrMgNO_4$	$C_{80}H_{96}Br_4Mg_4N_4O_{15}$
fw	398.58	1770.49
cryst syst	triclinic	triclinic
space group	*P*1	*P*1
color	colorless	colorless
a	9.399(2) Å	13.186(1) Å
b	9.858(2) Å	13.981(1) Å
c	11.583(2) Å	23.562(2) Å
α	72.152(3)°	97.387(1)°
β	87.777(3)°	92.529(2)°
γ	63.519(3)°	102.686(1)°
V	908.3(3) Å^3	4190.7(6) Å^3
Z	2	2
temp	173(2) K	173(2) K
γ	0.71073 Å	0.71073 Å
measured reflns	8130	29326
independent reflns	3154	14677
observed reflns	2744	10345
params	217	1029
restraints	66	238
R_{all}	0.0439	0.0767
R_{obs}	0.0337	0.0493
wR_{all}	0.0759	0.1520
wR_{obs}	0.0724	0.1400
GOF	1.029	1.037

Scheme 3

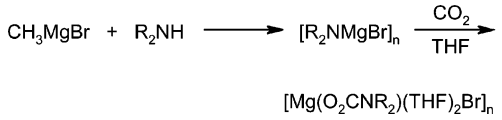

Results and Discussion

Compound **1** arises from the reaction of CO_2 gas with *N*-phenylanilidomagnesium bromide generated in situ by methathesis of methylmagnesium bromide with *N*-methylaniline, Scheme 3. The structure of **1**, Figure 1, shows the dimeric complex with two syn-syn-$\mu_{1,3}$ bridging *N*-phenyl-*N*-methylcarbamato ligands. Metrical parameters for **1** are presented in Table 2. Each magnesium ion is in a five-coordinated trigonal bipyramidal geometry as indicated by a τ[17] index of 0.82. The trigonal plane is composed of two oxygen donors from the carbamato ligands, and the bromide ligand. The axial coordination sites are occupied by two THF molecules. The Mg−O and Mg−Br bond distances are in

(12) Sheldrick, G. M. *Cell Now 1.0*; University of Göttingen: Göttingen, Germany, 2004.
(13) *SAINT 6.01 and 6.45*; Bruker Analytical X-Ray Systems: Madison, WI, 1998−2004.
(14) Sheldrick, G. M. *SADABS 1.0 and TWINABS 1.02* Bruker Analytical X-ray Systems, Madison, WI, 1996−2004.
(15) Brennessel, W. W.; Young, V. G., Jr. *STRIP REDUNDANT 1.3*; unpublished program, 2004.
(16) Sheldrick, G. M. *SHELXTL 6.12*; Bruker Analytical X-Ray Systems: Madison, WI, 2002.
(17) Addison, A. W.; Rao, T. N.; Reedijk, J.; van Rijn, J.; Verschoor, G. C. *J. Chem. Soc., Dalton Trans.* **1984**, 1349−1356.

Table 2. Important Structural Parameters in **1** and **2**

1

bond distances (Å)		bond angles (°)		torsion angles (°)	
Mg1−O1	1.923(2)	O1−Mg1−O2′	126.70(10)	O1−C1−N1−C3	3.6(4)
Mg1−O2′	1.964(2)	Br1−Mg1−O2′	117.22(7)	O1−C1−N1−C2	177.5(3)
Mg1−O3	2.121(2)	Br1−Mg1−O1	116.08(7)	C1−N1−C3−C8	−61.7(4)
Mg1−O4	2.098(2)	O3−Mg1−O4	175.59(9)	Mg1′−O2−C1−O1	35.1(4)
C1−O1	1.267(3)	O1−C1−O2	124.9(2)		
C1−O2	1.266(3)				
C1−N1	1.368(3)				
Mg1−Br1	2.5259(11)				
Mg1′···O1	3.28				
Mg1···O2	3.69				
Mg1···Mg1′	3.85				

2

bond distances (Å)				bond angles (°)		torsion angles (°)	
Mg1−O1	2.213(3)	C1−O1	1.276(4)	O2−Mg1−O1	60.11(10)	C1−N1−C5−C10	79.6(5)
Mg2−O2	2.189(3)	C1−O2	1.272(4)	O3−Mg1−O8	110.81(13)	C1−N1−C11−C12	61.7(5)
Mg1−O3	1.981(3)	C1−N1	1.353(5)	O1−C1−O2	119.8(3)	C2−N2−C27−C32	54.8(6)
Mg1−O8	1.968(3)	C2−O3	1.242(5)	O3−C2−O4	126.2(4)	C2−N2−C21−C22	64.2(6)
Mg1−O9	2.087(3)	C2−O4	1.273(5)	O5−C3−O6	127.0(3)	C3−N3−C47−C48	−79.9(5)
Mg1−Br1	2.7243(14)	C2−N2	1.394(5)	O7−C4−O8	126.5(3)	C3−N3−C41−C42	−92.2(5)
Mg2−O1	2.101(3)	C3−O5	1.259(4)			C4−N4−C61−C66	−80.0(5)
Mg2−O4	2.017(3)	C3−O6	1.259(4)			C4−N4−C67−C72	−44.3(6)
Mg2−O5	2.005(3)	C3−N3	1.392(5)				
Mg2−O10	2.096(3)	C4−O7	1.259(5)				
Mg2−O11	2.078(3)	C4−O8	1.262(5)				
Mg2−Br1	2.7450(14)	C4−N4	1.390(5)				
Mg3−O2	2.113(3)						
Mg3−O6	1.995(3)						
Mg3−O7	2.017(3)						
Mg3−O12	2.102(3)						
Mg3−O13	2.073(3)						
Mg3−Br1	2.7763(14)						
Mg1···Mg2	3.3250(18)						
Mg1···Mg3	3.3403(18)						
Mg2···Mg3	4.1250(19)						

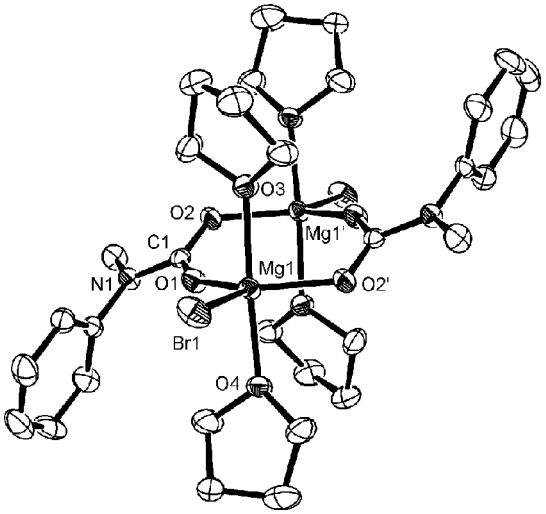

Figure 1. Molecular structure of **1** (50% ellipsoids). Only symmetry unrelated heteroatoms are labeled. Only one configuration for the disordered THF ligands is shown.

the expected ranges for this type of complex. The individual carbamate ligands are not symmetrically disposed between the two magnesium ions, but are slightly canted toward one, as shown by the shorter Mg1′···O1 distance (3.28Å) vs the Mg1···O2 distance (3.69Å). This is despite the nearly identical Mg−O1 (1.923(2)Å) and Mg−O2′ (1.964(2)Å) distances. The Mg1′−O2−C1−O1 torsion angle is 35.1(4)°, a consequence of the fact the C1 atom is displaced out of the plane of the $Mg_2(O_2C)_2$ core. The phenyl group in **1** is rotated substantially with respect to the NCO_2 plane, as shown by the C1−N1−C3−C8 torsion angle of −61.7(4)°. This precludes substantial delocalization of the nitrogen lone pair into the aromatic ring, a consequence of the strong π-electron withdrawing effect of the carboxyl group.

Table 3. Structural Parameters for Dinuclear Carbamatomagnesium and Carboxylatomagnesium Complexes $[Mg(O_2CR)(THF)_2Br]_2$

	R	Mg−O_A (Å)	Mg−O_B (Å)[a]	Mg−O_D (Å)	O−C−O (°)	Mg···Mg (Å)
1	N(Me)Ph	1.92	3.28	1.96	124.5	3.85
3a[b]	NEt_2	1.97	3.32	1.98	124.5	3.78
3b[b]	NEt_2	2.01	2.40	2.07	118.7	3.35
4[c]	N^iPr_2	1.96	2.36	2.04	118.8	3.28
5[d]	Ph	1.93	3.09	1.98	123.9	3.85

[a] For the $\mu_{1,3}$ complexes, *B* is defined as the shortest distance between the first Mg^{2+} and an oxygen coordinate to the second Mg^{2+}. [b] From ref 5. [c] From ref 4. [d] From ref 3.

Table 3 compares important metrical parameters for **1** with isostructural carbamatomagnesium and carboxylatomagnesium complexes from the literature.[3−5] The compounds in this table clearly belong to two classes, based on the metrical parameters illustrated in Scheme 2. Those having a Mg···Mg distance longer than 3.7 Å also have a distance *B* greater than 3.0 Å and an O−C−O angle θ greater than 123°. The new compound **1** belongs to this class, which are interpreted in terms of a syn-syn-$\mu_{1,3}$ bridged carbamatomagnesium core.

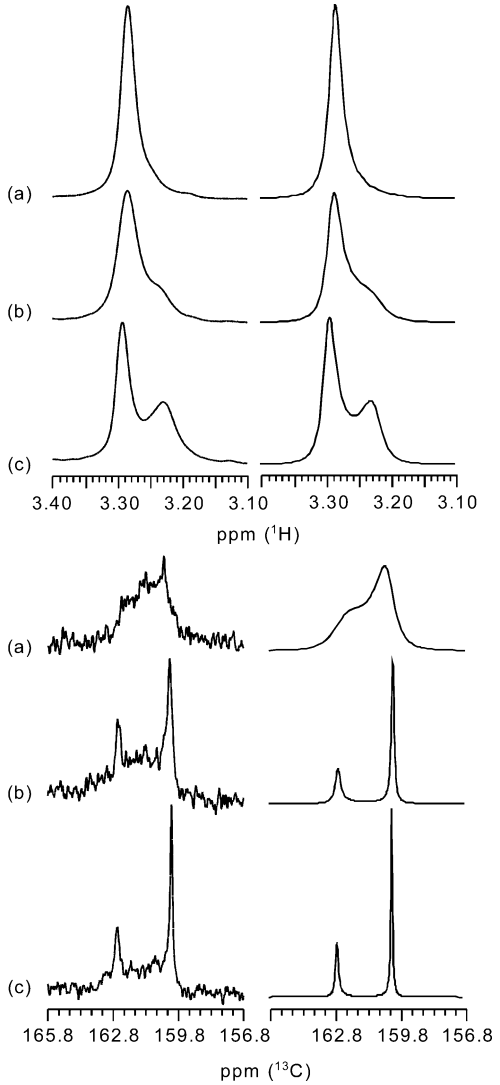

Figure 2. Top: Variable temperature ^{1}H NMR spectra ($CDCl_3$, 399.98 MHz) of **1** in the methyl region (left) and simulated spectra (right). Bottom: Variable temperature ^{13}C NMR spectra ($CDCl_3$, 100.58 MHz) of **1** in the carboxyl region (left) and simulated spectra (right). Solution contains 1% volume tetrahydrofuran. Compound **1** enriched with ^{13}C at the carboxyl carbon. (a) 25 °C, $\tau = 0.019$ s, $N_s = 0.33$, $N_r = 0.67$. (b) 10 °C, $\tau = 0.050$ s, $N_s = 0.33$, $N_r = 0.67$. (c) 0 °C, $\tau = 0.08$ s, $N_s = 0.38$, $N_r = 0.62$.

A Mg···Mg distance less than 3.4 Å is correlated with a distance B that is less than 2.5 Å and an angle θ markedly compressed to smaller than 120°. These are interpreted in terms of a syn-anti-$\mu_{1,1}$ bridging mode, in which the compression of the O−C−O angle results from the fact that the carbamato group is bidentate to one Mg^{2+} ion.

Complex **1** exhibits fluxional behavior in solution between 25 °C and 0 °C, as demonstrated by the temperature-dependent proton and ^{13}C NMR spectra in Figure 2. At room temperature, the ^{1}H NMR spectrum shows a single broad signal at 3.30 ppm arising from the *N*-methyl protons and the ^{13}C NMR spectrum shows a single broad resonance arising from the carboxyl carbon nucleus at 161.6 ppm. At 0 °C both of these signals decoalesce to yield two signals arising from the methyl protons and the carboxyl carbon, respectively. This behavior is indicative of a fluxional process between 25 °C and 0 °C that relates two distinct environments for the carbamato group. The variable temperature NMR spectra were modeled using a chemical exchange process relating two chemical sites having different equilibrium populations, with an exchange lifetime τ.[18] The good agreement between the exchange lifetimes obtained from the ^{1}H NMR and ^{13}C NMR data are consistent with line shapes arising from a common exchange process. Applying Eq 1, we were able to determine kinetic activation parameters for the forward and reverse rate processes giving rise to the dynamic NMR behavior.

Table 4. Kinetic Activation Parameters for Bridge-Mode Isomerization in $[Mg(O_2CR)(THF)_2Br]_2$ Complexes

complex	$\Delta H^{\ddagger}$ [a]	$\Delta S^{\ddagger}$ [b]	$\Delta G_{298}^{\ddagger}$ [a]
1	37[c]	−88[c]	63[c]
	37[d]	−85[d]	62[d]
3	45[e]	−50[e]	61[e]
5	43[e]	−46[e]	57[e]

[a] kJ/mol. [b] J/mol·K. [c] Activation parameters in the forward direction. [d] Activation parameters in the reverse direction. [e] Activation parameters are the same in the forward and reverse directions.

$$\tau = \frac{1}{2}\left(\frac{1}{k_f} + \frac{1}{k_r}\right) \quad (1)$$

An Eyring plot of $\ln(k/T)$ ($k = 1/\tau$) vs $1/T$ gives estimates for the activation parameters for bridge-mode isomerization in **1**, Table 4. These activation parameters are in the range reported for carboxylate shift dynamics in polynuclear carboxylatozinc complexes[11] and suggest that the fluxional NMR process in Figure 2 arises from interconversion of syn-syn-$\mu_{1,3}$ and syn-anti-$\mu_{1,1}$ bridge-mode isomers of **1**. For comparison, we also measured kinetic parameters for bridge-mode isomerization in the previously reported diethylcarbamato derivative **3**[5] and the closely related benzoate-bridged complex **5**,[3] Figures S1 and S2 (Supporting Information).[19] Analysis of **3** and **5** was simplified by the fact that the equilibrium constant for isomerization was essentially unity, so that $k_f = k_r$. In the case of **3**, the presence of bridge-mode isomers was previously confirmed by isolating and crystallographically characterizing both isomers of **3**.[5] Given the similarity in structure, we anticipated similar solution behavior for **1**, although we have been able to crystallize only the syn-syn-$\mu_{1,3}$ form in this case. The similarity in activation parameters in Table 4 is taken to suggest that a similar isomerization process is involved in all three systems. All three compounds have $\Delta S^{\ddagger} < 0$, indicating a transition state more ordered than the ground state. This suggests an isomerization mechanism that does not involve dissociation of a carbamato ligand and is more consistent with internal reorganization of the complex between the syn-syn-$\mu_{1,3}$ and syn-anti-$\mu_{1,1}$ forms as illustrated in Scheme 1. These data suggest that bridge-mode isomerism in the $[Mg(O_2CR)Br]_2$ system (R = alkyl/aryl/amino)is a general phenomenon.

Among known complexes of the $[Mg(O_2CNR_2)Br]_2[L]_4$ type, **1** is unique in having two different substituents on the

(18) Binsch, G. In *Dynamic Nuclear Magnetic Resonance Spectroscopy*; Jackman, L. M., Cotton, F. A., Eds.; Academic Press: New York, 1975; pp 45−81.
(19) Deposited in Supporting Information.

Scheme 4

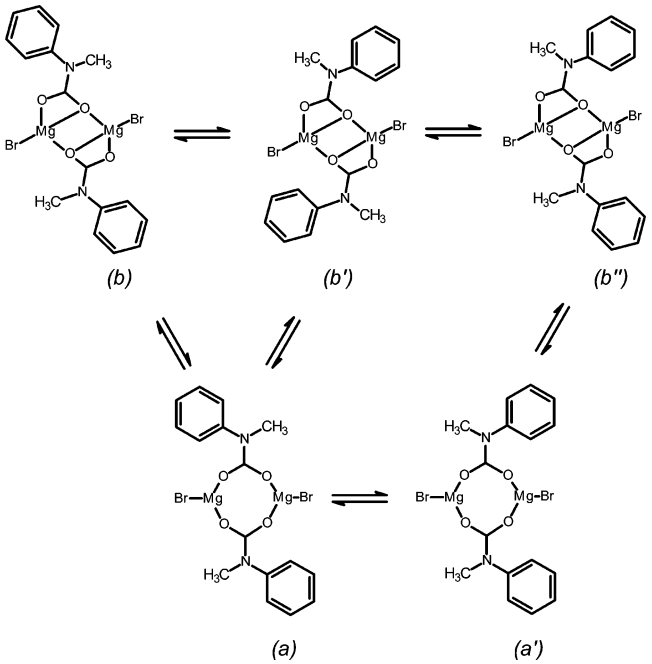

nitrogen atom. As a result, we have the possibility of C−N rotational isomers as well as bridge-mode isomers. As the sample is cooled to −50 °C, the ^{1}H NMR and ^{13}C NMR spectra increase in complexity, indicating the resolution of more than two exchanging species at temperatures below −10 °C, Figure S3 (Supporting Information).[19] We ascribe this new structure in the NMR spectrum to the resolution of C−N rotational isomers below 0 °C, which is superimposed onto the bridge-mode isomerism observed above 0 °C. This is generally consistent with hindered C−N rotation observed for carbamates and urethanes.[20] Consideration of all the possible rotational and bridge-mode isomers shows that there are two unique syn-syn-$\mu_{1,3}$ isomers (a and a′) that are related by rotation about one of the C−N bonds and that give rise to two chemically unique carbamato groups, Scheme 4. There also exist three possible syn-anti-$\mu_{1,1}$ isomers (b, b′, and b″) which collectively give rise to four chemically distinct carbamato ligands since the two carbamato groups in b″ are not equivalent. The vertical equilibria relate bridge-mode isomers, and the horizontal equilibria relate C−N rotational isomers. We clearly do not resolve all of these isomers at low temperature, and we have no means for assigning NMR signals to particular isomers in any event. However, the high-temperature and low-temperature dynamic NMR data for **1** may be qualitatively understood on the basis of Scheme 4 if the bridge-mode isomerization is rapid relative to C−N rotational isomerization.

(20) Deetz, M. J.; Forbes, C. C.; Jonas, M.; Malerich, J. P.; Smith, B. D.; Wiest, O. *J. Org. Chem.* **2002**, *67*, 3949−3952; Yamagami, C.; Takao, N.; Takeuchi, Y. *Aust. J. Chem.* **1986**, *39*, 457−463; Julia, S.; Ginebreda, A.; Sala, P.; Sancho, M.; Annunziata, R.; Cozzi, F. *Org. Magn. Reson.* **1983**, *21*, 573−575; Kornberg, N.; Kost, D. *J. Chem. Soc., Perkin Trans. 2* **1976**, 1661−1664. Yoder, C. H.; Komoriya, A.; Kochanowski, J. E.; Suydam, F. H. *J. Am. Chem. Soc.* **1971**, *93*, 6515−6518. Thompson, J. C.; Lemire, A. E. *J. Am. Chem. Soc.* **1971**, *93*, 1163−1165.

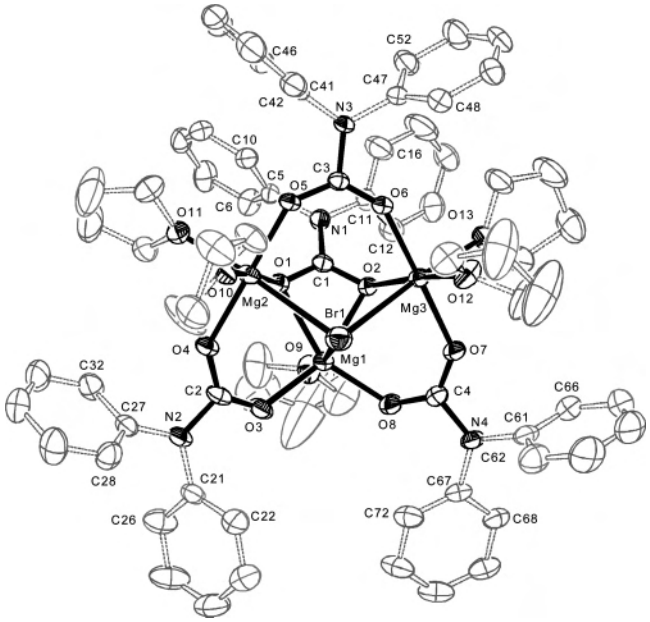

Figure 3. Molecular structure of **2** (50% ellipsoids). The Mg_3 core is in black and the phenyl groups and tetrahydrofuran ligands are in gray. Only one configuration for the disordered THF ligands is shown.

Compound **2** was prepared by a methodology similar to **1**, involving addition of CO_2 to Ph_2NMgBr prepared in situ. The structure of the cationic unit in compound **2** is shown in Figure 3. It consists of a trinuclear magnesium core supported by a pyramidal μ_3 bromide ion and four carbamato anions. The core has C_s point symmetry with the single mirror plane relating Mg2 and Mg3. The carbamato ligands containing C2 and C4 bridge the Mg1···Mg2 and Mg1···Mg3 vectors in a syn-syn-$\mu_{1,3}$ fashion and are related by the mirror symmetry as well. The Mg2···Mg3 vector is bridged by the ligand containing C3 in a syn-syn-$\mu_{1,3}$ fashion. The carbamato ligand C1 supports the core by bridging all three magnesium ions. It is coordinated to Mg1 in a bidentate fashion, and also bridges the Mg1···Mg2 and Mg1···Mg3 vectors in a syn-anti-$\mu_{1,1}$ fashion. The O1−C1−O2 angle of 119.8(3)° is substantially compressed relative to the three other carboxyl O−C−O angles, which are all greater than 126°. The C1−N1 distance of 1.353(5) Å is also systematically shorter than the other C−N distances. This suggests considerable charge polarization toward the O1 and O2 atoms, which is to be expected since each is bonded to two Mg^{2+} ions. All of the carbamato groups are planar, as expected, but the phenyl groups are rotated with respect to the carbamate planes, as shown by the torsion angles in Table 2 between 43.9° and 92.3°. Each Mg^{2+} ion is six-coordinated, with the inner coordination shell completed by tetrahydrofuran molecules. The bond distances and angles around the Mg2 and Mg3 ions are as expected for an octahedral center. Mg1 is six-coordinated but is otherwise highly distorted from an idealized octahedral environment as a result of the bidentate carbamato ligand. The O1−Mg1−O2 angle is only 60.11(10)° and the opposing O3−Mg1−O8 angle is correspondingly larger at 110.81(13)°. The counterion consists of a tribromomagnesiate ion solvated by one THF molecule to give a pseudo-tetrahedral $[(THF)Mg(Br)_3]^-$ ion. In solu-

Scheme 5

$$\underset{\mathbf{A}}{2\,[Mg(L)(THF)_2Br]_2} \rightleftharpoons \underset{\mathbf{B}}{[Mg_3(L)_4(THF)_5Br]^+[(THF)MgBr_3]^-} + 2\,THF$$

tion, compound **2** gives a complicated ^{13}C NMR spectrum in the carboxyl region between 158 and 166 ppm, and almost certainly indicates that the trinuclear structure of solid state **2** is not maintained in solution. The magnesium cation arising from the $[(THF)Mg(Br)_3]^-$ may serve to catalyze ligand exchange reactions of the trinuclear cluster, and may also condense with the Mg_3 cluster to give other magnesium complexes.

The very different structural motifs adopted by **1** and **2** in the crystalline state is surprising given the close compositional relationship between the two compounds. In solution, the two motifs can be related by the equilibrium in Scheme 5, where the core compositions of **A** and **B** differ only by the dissociation of two inner-sphere THF molecules in the latter. The preference for **A** or **B** in principle could arise by changing the solvent composition, with a decrease in the THF content favoring dissociation of solvent molecules. This could lead to the formation of the trimagnesium species **B** as the system re-equilibrates to fill the unoccupied bond valence of the magnesium ions through ligand bridging interactions that result in an increase in complex nuclearity. However, we find no evidence from NMR spectroscopy that compound **2** reverts to form **A** in the presence of excess THF, nor do we observe that compound **1** condenses to form **B** in poorly coordinating solvents. Therefore, we ascribe the observed structural preferences in the heteroleptic bromomagnesium complexes **1** and **2** to effects relating to the substitution of the *N*-methyl group in **1** for an *N*-phenyl group in **2**.

Among those carboxylate bridged complexes included in the class II bridged carboxylate complexes,[6] there is a linear correlation between the parameters *B* and *D*, Scheme 2, and it is shown in Figure 4 that the syn-anti-$\mu_{1,1}$ bridged carbamato complexes fall on this correlation. Indeed, they demarcate an extreme in the metrical parameters of this particular class, having the largest value for *B* and the correspondingly smallest value for *D*. Shifting to the syn-syn-$\mu_{1,3}$ bridging mode results in a decrease in *D* and a large increase in *B* and these compounds are best categorized along with the class III bridging carboxylate complexes. Compounds **1**, **3**, and **5** constitute rare examples in which dinuclear complexes exhibit dynamic bridge-mode isomerization reminiscent of the carboxylate shift, although examples have been reported in complexes of higher nuclearity.[11] The only example among paramagnetic complexes interprets temperature-dependent ^{19}F NMR of a sterically hindered diiron(II) complex in terms of a bridging to terminal-bidentate shift for two carboxylate ligands.[21] These examples provide a sufficient basis to conclude that dynamic carboxylate shifts may be a general phenomenon in the solution chemistry of polynuclear metal carboxylate and carbamate complexes. The incomplete picture of the solution behavior of these compounds provided by single-crystal

(21) Lee, D.; Lippard, S. J. *Inorg. Chem.* **2002**, *41*, 2704−2719.

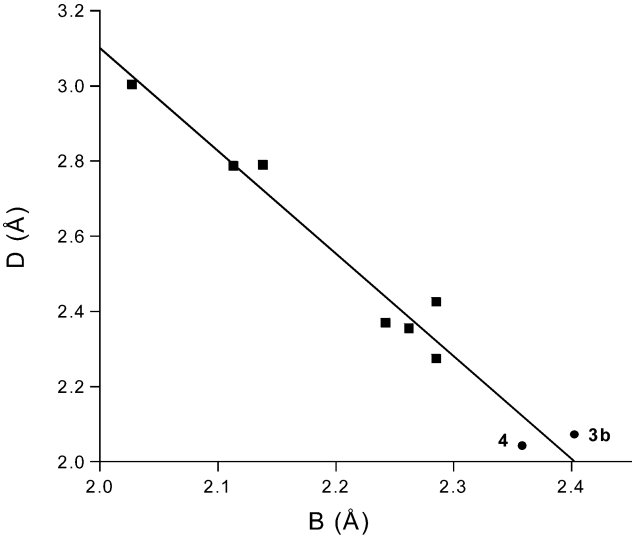

Figure 4. Correlation of *D* with *B* for carboxylate and carbamate-bridged metal complexes. (■) Data from ref 6. (●) Data for **3b** from ref 5. Data for **4** from ref 4. Å.

X-ray structures should inspire caution when spectroscopic data is measured on carboxylate bridged complexes in solution, but is interpreted in terms of a structure based on solid state X-ray diffraction data. This is particularly true for methods that are strongly dependent on metal−metal interactions, such as EPR spectra or magnetic measurements, since spin−spin coupling constants can be very dependent on the specifics of the moiety bridging two metal ions.

The carboxylate shift may be an important kinetic process in dinuclear enzyme active sites. Crystallographic studies of an F208A/Y122F mutant of the R2 subunit of ribonucleotide reductase shows that binding of azide to the dinuclear iron(II) center results in the shift of a glutamate ligand, E238, from a syn-syn-$\mu_{1,3}$ to syn-anti-$\mu_{1,1}$ bridging mode in which E238 is also a bidentate ligand to one iron(II).[7] An important consequence of this shift is that the Fe···Fe distance is decreased by about 0.4 Å from 3.8 Å to 3.4 Å, which is in line with the Mg···Mg compression in the dimagnesium complexes upon shifting from the syn-syn-$\mu_{1,3}$ to syn-anti-$\mu_{1,1}$ bridging mode. The Fe···Fe distance in the oxidized (met) R2 is 3.3 Å,[8] suggesting that compression of the Fe···Fe distance by carboxylate shift is critical to oxidation of the center. This is supported by subsequent crystallographic studies on the dimanganese(II) substituted R2,[9] which show that oxidation of the Mn^{II}_2 center by one electron gives a $Mn^{II}Mn^{III}$ site in which E238 has shifted to a syn-anti-$\mu_{1,1}$ mode, with the expected short Mn···Mn distance of 3.4 Å. This prompts the hypothesis that the carboxylate shift dynamics may actually precede oxygen binding to R2, with the E238 syn-anti-$\mu_{1,1}$ bridging mode providing a more favorable coordination environment for ligation of O_2. There is also good evidence for this type of dynamic bridging carboxylate motion in oxygen binding by the related diiron center in methane monooxygenase.[10] It is therefore important to develop a more sophisticated understanding of the carboxylate shift as a dynamic process that may affect the function of dinuclear metalloenzymes.

Acknowledgment. The National Science Foundation is acknowledged for a grant to M.T.C. (CHE-9985266), and for contribution toward the purchase of single-crystal instrumentation used in this study (CHE 9808440). Elizabeth Sanchez and Dr. Mike Williams are acknowledged for assistance in collecting the low-temperature NMR data.

Supporting Information Available: Two crystallographic data files in CIF format for **1** and **2**, with details of crystallographic refinement; Figures S1−S3 showing temperature-dependent NMR spectra; details of the collection of temperature-dependent NMR data; details of the synthesis of {^{13}C}**5**. This material is available free of charge via the Internet at http://pubs.acs.org.

IC048442P